Comparing lightning observations of the ground-based EUCLID network and the space-based ISS-LIS

Dieter R. Poelman[1], Wolfgang Schulz[2]

[1]Royal Meteorological Institute of Belgium, Brussels, Belgium
[2]OVE-ALDIS, Vienna, Austria

Correspondence to: Dieter R. Poelman (dieter.poelman@meteo.be)

Abstract. The Lightning Imaging Sensor (LIS) on the International Space Station (ISS) detects lightning from space by capturing the optical scattered light emitted from the top of the clouds. On the other hand, the ground-based European Cooperation for Lightning Detection (EUCLID) makes use of the low-frequency electromagnetic signals generated by lightning discharges to locate those accordingly. The objective of this work is to quantify the similarities and contrasts between the latter two distinct lightning detection technologies by comparing the EUCLID cloud-to-ground strokes and intracloud pulses to the ISS-LIS groups, in addition to the correlation at the flash level. The analysis is based on the observations made during March 01, 2017 and March 31, 2019 within the EUCLID network and limited to 54° north. A Bayesian approach is adopted to determine the relative and absolute detection efficiencies (DE) of each system. It is found that the EUCLID relative and absolute flash DE improves by approximately 10 % towards the center of the EUCLID network up to a value of 56.3 % and 69.0 %, respectively, compared to the averaged value over the full domain, inherent to the network geometry and sensor technology. On the other hand, the relative and absolute ISS-LIS flash DE over the full domain is 48.4 % and 71.3 %, respectively, and is somewhat higher than the values obtained in the centre of the EUCLID network. The behavior of the relative DE of each system in terms of the flash characteristics of the other reveals that the greater the value the more likely the other system detects the flash. For instance, when the ISS-LIS flash duration is smaller or equal to 200 ms, the EUCLID relative flash DE drops below 50 %, whereas it increases up to 80 % for ISS-LIS flashes with a duration longer than 750 ms. Finally, the distribution of the diurnal DE indicates higher (lower) ISS-LIS (EUCLID) DE at night, related to an increased ISS-LIS:EUCLID flash ratio at night.

1 Introduction

Lightning processes in the cloud and from cloud-to-ground involve the formation of channels carrying tens of kiloamperes of electric current with temperatures as high as 30,000 K. Those processes are accompanied by intense radiation in the optical frequency range with the peak power typically being of the order of 10^9 W (Christian et al., 1989). These optical emissions are a result of dissociation, excitation, and subsequent recombination of various atmospheric constituents as a result of the sudden intense heating, and primarily occur at discrete atomic lines. Satellite-based optical imagers operating in the visible and near infrared frequency ranges record these optical emissions. The geolocation is carried out by using geometric projection of the images taken from space. In the seventies of last century, different satellite programs started to use various

optical sensors to measure lightning, e.g., Vorpahl J.A. et al. (1970), Sparrow & Ney (1971) and Turman (1978). Due to the limited technology at this time, these satellite-based sensors had location accuracies of the order of hundreds of kilometers due to the low spatial resolution of the optical imagers and a detection efficiency of less than 2 %. In 1995 the OV-1 (MicroLab 1) satellite carrying the optical transient detector (OTD) was launched, followed by the TRMM satellite carrying the lightning imaging sensor (LIS) in 1997. OV-1 orbited at an altitude of 750 km, whereas TRMM originally rotated at an altitude of 350 km and being changed to 400 km after 2001 (Cecil et al., 2014). The latter two satellites had a large field of view (fov) of 1300 x 1300 km and 600 x 600 km for OTD and LIS, respectively. Those optical imagers measure the signals emitted at 777.4 nm, associated with the dissociation of molecular oxygen into atomic oxygen due to intense heating produced by lightning processes. Data from such sensors typically consist of the time of occurrence of the lightning discharge, its latitude, and longitude. The spectral energy density for each event is also available (Koshak, 2010), but interpretation of these measurements is complicated because the optical properties of the path between the emission and the measurement point vary. Since no relationship exists between the peak optical radiance measured by such sensors and the peak currents of lightning discharges, estimated peak current and polarity of lightning discharges are not reported by satellite-based lightning sensors. OTD and LIS have a location accuracy of about ten to a few tens of kilometers and a temporal resolution of several milliseconds, e.g., Boccippio et al. (2000). It detects emissions from both cloud and cloud-to-ground discharges but cannot distinguish between the latter two. Total flash detection efficiency for LIS during day and night is estimated to be 70 % and 88 %, respectively, and approximately 38 % and 52 %, respectively, for OTD, see Boccippio et al. (2002) and Cecil et al. (2014). It is important to note that, similar to VHF lightning mapping systems, optical imagers are able to map the full spatial extent of flashes, although with poorer temporal and spatial resolution, and hence may be viewed as lightning mapping systems. Since these optical imagers on low earth orbiting satellites observe a given location on the Earth's surface for a limited time; typically around 90 seconds to a few minutes, they can only take snapshots of thunderstorms and cannot monitor them as they develop and evolve.

Generally, for all applications of lightning data it is important to know the performance of the employed lightning location system (LLS). The performance characteristics of lightning location systems are determined by their ability to geolocate lightning discharges with high location accuracy (LA), high detection efficiency (DE), a low false detection rate and to report various other features of the lightning discharge correctly. Different methods or a combination of methods may be used to validate the performance characteristics of different types of lightning locating systems, see Nag et al. (2015). To get information about performance variations over large spatial regions of ground based LLS, data of those systems were compared to data from TRMM-LIS. During the last years several papers provided additional insights in the performance of ground based networks with such an analysis, e.g., the WWLLN (Rudlosky & Shea, 2013), the NLDN (Zhang et al., 2016), the ENTLN (Rudlosky, 2015), the ATDnet (Enno et al., 2018) and the GLD360 (Rudlosky et al., 2017). One have to keep in mind that during the last years the performance of the ground based networks improved significantly and therefore the analyses of data between 2008 and 2014 may not provide information about the current LLS performance.

65 In April 2013 it was decided that a LIS, built as the flight spare for the TRMM satellite, should be put on the International Space Station (ISS) and almost 4 years later (March 2017) the instrument started recording data. The data of this sensor, called ISS-LIS, was analyzed in Erdmann et al. (2019) for the time period March 2017 to March 2018. They compared for the first time, although in a small part of Europe, ISS-LIS data to the low-frequency LLS of Météorage and the lightning mapping array SAETTA (Coquillat et al., 2019) over the northwestern Mediterranean Sea near Corsica. In this paper the

70 performance of EUCLID (EUropean Cooperation for LIghtning Detection), a ground based LLS similar to the LLS of Météorage, will be evaluated relative to the ISS-LIS data over an extended time period and larger area in Europe as compared to Erdmann et al. (2019) This work is timely, given that the Meteosat Third Generation (MTG), which has a lightning imager (LI) on board, is going to be launched in two years.

2 Data

75 ### 2.1 EUCLID

Starting in 2001 the European Cooperation for Lightning Detection (EUCLID) geolocates cloud-to-ground (CG) strokes and intracloud (IC) pulses through a combination of time-of-arrival (TOA) and direction finding (DF) techniques. The EUCLID cooperation is special in the sense that it combines raw sensor data in real-time of independent lightning location systems ─ either managed by National Meteorological Services (NMS) or by private companies ─ within a single processor. This is

80 possible since all of the sensors operate in the same low-frequency (LF) range and are from the same manufacturer, i.e., Vaisala. The central processor of EUCLID adopts individually calibrated sensor gains and sensitivities to account for any local sensor site conditions. Those values can differ from the ones used by the local LLS provider due to the implicit higher redundancy in EUCLID as a result of the participation of additional sensors located outside the national borders in a neighboring country. Hence, it assures that the resulting lightning data are of high and nearly homogeneous quality

85 throughout Europe. The performance of EUCLID has been frequently tested over the years in terms of its LA, DE and peak current estimation. Those performances have been determined either from direct lightning measurements at the Gaisberg Tower (GBT) (Diendorfer et al., 2009), Peißenberg tower in Germany (Heidler & Schulz, 2016) and Säntis tower in Switzerland (Romero et al., 2011; Azadifar et al., 2016) as well as from video and E-field records collected in different regions within Europe (Poelman et al., 2013; Schulz et al., 2016). The current LA is in the order of 100 m based on the

90 location error directly measured at the GBT and based on video and E-field recordings within the majority of the network. The DE for negative CG strokes/flashes reaches 70/96 % based on GBT data and is determined to be 84/98 % using video and E-field records. On the other hand, the DE for positive discharges is greater than 84 % and 87 % for CG strokes and CG flashes, respectively (Schulz et al., 2016). Finally, IC DE has been validated during the HyMeX experiment (Ducrocy et al., 2013; Defer et al., 2015) in the south of France (Schulz et al., 2014; Pédeboy et al., 2014). For this purpose, EUCLID

95 observations were matched to the observations made by the Lightning Mapping Array "HyLMA". It is found that the DE of isolated IC flashes, i.e., pure IC flashes without any CG stroke in it, has a large variation ranging from 10 % up to 67 % from

one thunderstorm to another. This variability is mainly attributed to differences in the vertical extent of the IC flash and to the flash rates during a storm. Regarding the peak current estimates, EUCLID tends to overestimate those slightly with respect to the currents measured at the GBT with a median error of 4 %. More information regarding the performance and observations by the EUCLID network is found in Schulz et al. (2016) and Poelman et al. (2016).

2.2 ISS-LIS

The Lightning Imaging Sensor (LIS) aboard the International Space Station (ISS) is identical to the LIS used on the Tropical Rainfall Measuring Mission (TRMM) satellite which was operational from 1999 to 2015. LIS on ISS was installed in February 2017 with an intended mission lifespan of two years and collects lightning data from that point onward from a low earth orbit (LEO) at an altitude of about 408 km; similar to the altitude of the TRMM satellite after 2001. The LIS sensor combines a wide fov lens with a narrow-band interference filter of 1 nm centered on the strong oxygen triplet emission line at 777.4 nm. In addition, LIS employs an optical staring imager composed of a 128 x 128 charged coupled device (CCD) array with a sampling rate of approximately 500 frames per second. Although latitudinal coverage is expanded poleward to 54° due to a larger orbit inclination (55° instead of 35° for the TRMM satellite) the performance characteristics of ISS-LIS are similar to that of TRMM-LIS. This means that the electrical activity within thunderstorms is detected with a resolution of 4 km at nadir and increases somewhat towards the edge of the measurement region, with a swath width of about 650 km of the Earth's surface. Hence, due to the continuous movement of the ISS with an orbital speed of approximately 7 km/s, lightning observations over a specific region lasts no longer than 90 seconds per overpass. When a lightning discharge occurs, the optical signal scatters throughout the cloud. In almost all of the cases, except in the unlikely case the cloud is extremely optically thick, this results in an extended area being light up on the top of the cloud when viewed from space. At the moment a pixel on the CCD array receives this optical pulse, the signal is compared to the dynamically changing detection background threshold. Once this threshold is exceeded, the processor identifies the illuminated pixel as a LIS event. It is important to note that a LIS event has no counterpart when compared to the observations made by a ground-based LLS such as EUCLID. However, the collection of LIS events from adjacent pixels during the same 2 ms frame integration time, defined as a LIS group, is comparable with either a CG stroke or cloud pulse. Note that the ISS-LIS group location is the radiance-weighted centroid of all the events within the respective group (Mach et al., 2007). In its turn, groups are clustered within a flash when the spatial and time criteria of 5.5 km and 330 ms, respectively, are met. In contrast to EUCLID, LIS is not able to distinguish between CG and IC lightning. Nevertheless, Boccippio et al. (2002) estimated an upper bound for the TRMM-LIS total flash DE of 88 ± 9 %.

In this work, we make use of the non-quality controlled ISS-LIS dataset (Publication date: 2019-08-19, Version 1, Processing level 2) made available by the NASA Global Hydrology Resource Center DAAC (Blakeslee, 2019). The non-quality controlled label is somewhat misleading since the data does include quality information in the form of alert/warning flags, however some improvements to the algorithm creating the ISS-LIS data files is still ongoing. The main issue being the sensitivity of ISS-LIS compared to TRMM-LIS, with the DE for ISS-LIS on the order of 5% less than the DE for TRMM-

130 LIS (R. Blakeslee, 2019 GLM Annual Science Team Meeting, Huntsville), impacting to some degree the DE values presented in this paper. The data includes information on geolocated and time-tagged lightning events, groups and flashes, orbit statistics and metadata. For more in depth information on the LIS instrument, the interested reader is referred to Christian et al. (1989), Blakeslee et al. (2014) and Blakeslee & Koshak (2016).

3 Methodology

135 In this paper EUCLID and ISS-LIS lightning observations are correlated using data from March 01, 2017 until March 31, 2019, as observed within the EUCLID domain and limited to 54° north. ISS-LIS detects optically bright discharges, such as return strokes and in-cloud discharges inducing a rapid change in the electric field (Goodman et al., 1988). Those rapid changes in the electric field are exactly the features detected by EUCLID. Hence, the fundamental unit of ISS-LIS, i.e., groups, and EUCLID, i.e., CG strokes and IC pulses, largely correspond to the same physical process and are therefore

140 directly comparable (Bitzer et al., 2016). Additionally, the comparison will be performed as well on the artificial derived flash level.

The approach taken in this work has been applied and described in detail in Rubinstein (1994) and Bitzer et al. (2016), in which a probabilistic method is used to estimate the relative and absolute detection efficiencies of both systems under investigation. The concepts are briefly defined hereafter.

145 Neither EUCLID nor ISS-LIS observe all the lightning activity that actually occurred at a given moment in time. Hence, let S be the set of all occurred lightning discharges and A and B the set of discharges detected by ISS-LIS and EUCLID, respectively, as illustrated in Figure 1. It is possible that both of the systems contain some false alarm detections and therefore fall outside S. However, those false alarms constitute roughly 1 % of the total amount of discharges detected by EUCLID (Poelman et al., 2017), whereas the false event rate requirement for LIS is set to be less than 5 %. Hence, the latter

150 has a minor influence on the final outcome. The system dependent relative detection efficiencies can be expressed as:

$$P(A \mid B) = \frac{n_A \cap n_B}{n_B} \tag{1}$$

$$P(B \mid A) = \frac{n_A \cap n_B}{n_A} \tag{2}$$

with n_A and n_B the amount of discharges detected by system A and B, respectively, and $n_A \cap n_B$ the intersection containing

155 discharges detected by both systems. Thus P(A|B) represents the conditional probability that LLS A detects a discharge relative to LLS B, and vice versa in case of P(B|A). In addition, the true detection efficiency, for example of system A, reads as:

$$P(A) = \frac{n_A}{n_S}, \tag{3}$$

whereas the actual amount of occurred discharges n_S is not known a priori. Therefore, the estimated absolute detection efficiencies (ignoring false detections) can be calculated in the following way:

$$P(A) = \frac{n_A}{n_S} \leq \frac{n_A}{n_A + n_B - n_A \cap n_B} \tag{4}$$

$$P(B) = \frac{n_B}{n_S} \leq \frac{n_B}{n_A + n_B - n_A \cap n_B} \tag{5}$$

Since the number of detections in S, n_S, is larger than the unique set of combined discharges in A and B, the estimated absolute DE is an upper limit of the true detection efficiency. In order to precisely calculate the above detection efficiencies, only those EUCLID discharges that occurred within the ISS-LIS fov, n_B, need to be taken into account. To this end, the corner points of two consecutive ISS-LIS fovs, separated by roughly 35 seconds, are extrapolated to every second to increase accuracy. Then, for each second the EUCLID detections are extracted within the respective fov. As an example, ISS-LIS flashes and EUCLID CG and IC flashes are plotted on top of the ISS-LIS fov in Fig. 2. This is the biggest difference compared to the future MTG-LI observations from a geostationary orbit. Next, the individual EUCLID CG strokes and IC pulses are correlated in time and space with the ISS-LIS groups in order to retrieve the amount of overlapping detections. A match is found when the temporal and spatial criteria of 10 ms and 20 km, respectively, are fulfilled. Those particular criteria have been used in similar inter-comparison studies such as Franklin (2013), Bitzer et al. (2016) and Zhang et al. (2016; 2019). Note that for the stroke/group DE comparisons one ISS-LIS group can be matched to several EUCLID strokes/pulses and vice versa, but for time/location accuracy comparisons only the closest discharge in space is used. At the flash level, matching is somewhat more complicated due to the fact that EUCLID and ISS-LIS have their own specific flash clustering algorithms. For the flash analysis, EUCLID strokes/pulses are matched to ISS-LIS groups using a larger temporal (100 ms) and spatial (30 km) criterion to account for the fact that a flash can consist out of different discharges spread over some time interval. Subsequently, the strokes/pulses and groups are traced back to the respective flash it belongs to. Thus, a matched flash can have one or multiple matched discharges or groups. Be aware that since the flash grouping algorithms for EUCLID and ISS-LIS are different, the matched flash count is slightly different depending on whether EUCLID or ISS-LIS data is used as a reference for the matching algorithm. Hence, to account for this difference a scaling factor is applied in the same way as presented in Zhang (Zhang, 2019, p.140-141). Additionally, the absolute DE values at the level of groups/strokes are not relevant since the number of groups per LLS report is very large; artificially increasing the ISS-LIS group absolute DE value. Therefore, absolute DE values are only presented at the flash level in this study.

4 Results

4.1 EUCLID stroke/pulse and ISS-LIS group level

In Fig. 3 the spatial distribution of the IC:CG ratio, observed by EUCLID, is plotted for IC pulses and CG strokes, as well as at the flash level. Only data within the EUCLID domain as indicated by the dashed polygon and cut off at 54° north to account for the ISS-LIS latitudinal coverage are used for quantitative analysis in this work. The geographic spread does not reflect the actual IC:CG occurrence within Europe, but mainly highlights areas where EUCLID is more capable detecting IC activity over others due to sensor technology. Not surprisingly, the highest IC:CG ratios are found in regions where the baseline between LS700x sensors is small and drops off towards the south and east of the domain where mainly IMPACT sensors were installed during the period of investigation. Additionally, during this time period, in the south of Italy and in Spain significant communication problems deteriorated the results. The mean IC:CG stroke (flash) ratio over the entire region is 2.6 (1.9) and increases to 4.1 (2.8) within the rectangle highlighted in white. The rectangle highlighted in white in Fig. 3 will be referred to as the centre of the EUCLID network throughout the paper. The mean IC:CG flash ratio in the centre of the network is comparable to the values observed by the U.S. National Lightning Detection Network (NLDN) in various parts throughout the contiguous United States as presented by Medici et al. (2017). Since EUCLID observes most of the IC pulses in the centre of the network, in the remainder of the paper results will be presented for the full domain, as well as for the centre.

The distance offset Δd in one kilometre intervals between matched EUCLID strokes/pulses and ISS-LIS groups is indicated in Figure 4 and expressed in percentage of occurrence. A steep rise is observed up to 2-3 km, followed by a steady decrease for the larger distance offsets. The mean (median) location difference is 5.7 km (4.8 km) corresponding to approximately two pixels in the ISS-LIS CCD imager. This result is in line with previous findings as presented in Bitzer et al. (2016) and Zhang et al. (2019) who compared LIS group locations with comparable ground-based LLS. Towards the centre of the EUCLID network, the mean and median distance offset drops by 180 m and 200 m, respectively. This is not surprising since shorter baselines amongst the sensors in this region and the use of sensor based onset time calculation lead to a better location accuracy and hence better correspondence with the LIS group positions.

Similar to the distance offset, the timing differences Δt, calculated here as $t_{ISS-LIS} - t_{EUCLID}$, can be measured between matched discharges of both systems. The distribution of the time offset between matched ISS-LIS groups and EUCLID strokes/pulses is indicated in Figure 5. A positive (negative) value indicates that the ISS-LIS group occurred later (earlier) than the EUCLID match. It is found that the distribution peaks sharply around ±1 ms, with a positive mean (median) time offset of 0.23 ms (0.11 ms). Thus, on average a EUCLID stroke occurs first. Nonetheless, the majority of the timing differences fall inside the ISS-LIS timing accuracy set by the frame integration time of 2 ms. Unlike for the distance difference, the time offset does not differ within the EUCLID domain.

The estimated peak current of matched EUCLID CG strokes (solid line) and IC pulses (dashed line) are correlated with the ISS-LIS group radiance in Figure 6. Note that positive discharges with peak currents smaller than 10 kA are likely to be

misclassified as CG strokes because those are more likely to be of intracloud nature (Cummins et al., 1998; Wacker & Orville, 1999a;b; Jerauld et al., 2005; Orville et al., 2002; Biagi et al., 2007). Hence, positive CG strokes below 10 kA are all categorized as IC pulses and therefore no data for positive CG below 10 kA exist. Additionally, the largest positive IC pulse in the EUCLID dataset has an estimated peak current of 28.8 kA, limiting the positive IC pulse curve in the plot. In general,

225 higher peak current signals observed by EUCLID correspond with higher ISS-LIS group radiances. At larger absolute peak current values, i.e., $|I_p| \geq 20$ kA, the correlation becomes more variable. However, the latter is an artefact of the sample size, as indicated by the grey curve in the plot.

Finally, relative detection efficiencies can be calculated using the formulas described in Sect. III. The results for the full domain and the centre are listed in Table 1. It follows that the ISS-LIS group relative DE, i.e., P(ISS-LIS|EUCLID), is

230 36.5 %, while it is 14.7 % in case of P(EUCLID|ISS-LIS) over the full domain. In the centre of the EUCLID network P(ISS-LIS|EUCLID) is 36.6 %, while P(EUCLID|ISS-LIS) increases to 20.0 %. Those values are comparable with the relative detection efficiency values presented in Zhang et al. (2016), correlating NLDN detections with TRMM-LIS observations in 2013 over the CONUS, although P(TRMM-LIS|NLDN) was somewhat higher at 52.9 %. A possible explanation of the lower P(ISS-LIS|EUCLID) found in this study compared to P(TRMM-LIS|NLDN) in Zhang et al. (2016) is the advancement

235 of the LS700x technology in detecting IC pulses in between 2013 and the period 2017-2019 used in this study. Thus, in this work the EUCLID dataset contains more IC pulses, which have no counterpart in the ISS-LIS observations.

4.2 Flash level

The spatial distribution of the EUCLID and ISS-LIS flash counts is indicated in the upper plots of Figure 7, while the lower

240 plots show the geographic spread of the absolute flash detection efficiencies P(EUCLID) and P(ISS-LIS). The overall spatial behavior of the flash counts is similar between the two detection systems. However, the biggest difference in flash counts is found to be outside the center of the EUCLID network, especially over Spain, Italy and the Mediterranean Sea, where ISS-LIS outperforms EUCLID in terms of the amount of detections. For those regions the same comment applies as for the IC:CG ratio above, namely that this issue is related to the communication problems in those regions. Table 2 summarizes the

245 relative and absolute DEs within the full domain and in the centre of the EUCLID network. It is found that P(ISS-LIS|EUCLID) is 48.4 % overall and 48.0 % in the center of the network, while Zhang et al. (2016) found P(TRMM-LIS|NLDN) to be 68.3 %. Similar as in Section 4.1, the significant smaller average sensor baseline of the EUCLID network compared to the NLDN leads to an increased IC flash component in the EUCLID observations without any counterpart in the ISS-LIS flash observations, hence leading to a lower relative ISS-LIS DE in this work. On the other hand,

250 P(EUCLID|ISS-LIS) increases from 45.5 % overall to 56.3 % in the center of the network. The latter result is in line with the 48.7 % found in Zhang et al. (2016). An extra region is outlined in Figure 7 covering Corsica, corresponding with the region investigated by Erdmann et al. (2019) in which ISS-LIS flashes are matched against those observed by the ground-based Météorage network during an approximately 1-year period from March 1, 2017 until March 20, 2018. Applying analogue

flash matching criteria as in Erdmann et al. (2019) over the Corsica area, i.e., strokes/pulses are matched to ISS-LIS groups using a 1.0 s temporal and 20 km spatial criterion, P(ISS-LIS|EUCLID) becomes 59.7 % in this study, being similar to the 62.4 % found in Erdmann et al. (2019). Furthermore, Erdmann et al. (2019) found P(Météorage|ISS-LIS) to be 83.3 % over Corsica, and a similar value is found in this work with P(EUCLID|ISS-LIS) being 82.9 %. The absolute DE of ISS-LIS, P(ISS-LIS), is ≤71.3 % overall and drops to 66.1 % in the center of the EUCLID network, being somewhat smaller than the 81.5 % in Zhang et al. (2016). P(EUCLID) is 59.4 % overall and increases to 69.0 % in the center of the network, while it is 58.2 % in Zhang et al. (2016) in case of the NLDN. Smaller baselines in the center of the EUCLID network lead to a better P(EUCLID), whereas the full domain includes oceans and regions with larger baselines. Additionally, note that in Zhang et al. (2016), the NLDN observations used were restricted to the areas where the NLDN detection efficiency is highest. Hence, P(ISS-LIS) and P(EUCLID) of 66.1% and 69.0 %, respectively, in this work should be compared to P(TRMM-LIS) and P(NLDN) of 81.5% and 58.2 %, respectively, in Zhang et al. (2016). Taking into account the fact that ISS-LIS is somewhat less sensitive compared to TRMM-LIS, would bring the latter values a bit more in line with each other. From Figure 7 it is found that P(ISS-LIS) is highest outside the center of the EUCLID network, while it is the opposite in case of P(EUCLID). However, contrary to what is found in this study, the absolute DE for ISS-LIS should be uniform over the entire region, since it is highly unusual to expect a geographic dependence. It is believed that the spatial dependence is related to the limit of the Bayesian algorithm using only two networks. Probably making use of additional networks would make it disappear.

Average characteristics of all ISS-LIS flashes, those observed (matched) and not observed (unmatched) by EUCLID are listed in Table 3, while Figure 8 provides relative detection efficiency values as a function of those characteristics. From Table 3, it is found that the duration of ISS-LIS flashes is longer by a factor of 1.5 for those that have a match with a EUCLID flash compared to those not observed by EUCLID. Additionally, Fig. 8a demonstrates an increasing trend in the EUCLID flash DE with increasing flash duration. For flashes lasting longer than about 750 ms, the flash DE is stable around 60 % averaged over the full domain and increases further by about 20 % in the center of the EUCLID network. On average, ISS-LIS flashes consist of 8.6 groups, while matched flashes contain 10.7 groups and drops to 7.2 groups per flash for the unmatched flashes. Fig. 8b indicates a sharp increase in the EUCLID flash DE for ISS-LIS flashes comprising of up to about 10 groups, followed by a moderate rise in flash DE for flashes containing up to 30 groups. ISS-LIS flashes with more than 30 groups have the highest probability to match a EUCLID flash, resulting in a EUCLID flash DE between 60 %-80 %. A similar behavior is found when looking at the maximum number of events per group (MNEG), which has been plotted as well in Fig. 8b. Examining the behavior as a function of amount of events per flash, an analogue trend is observed compared to the previously examined behavior of groups per flash. Flashes containing 75 events or more boost the EUCLID flash DE up to 80 % in the center of the EUCLID network as depicted in Figure 8c. Fig. 8d demonstrates an identical behavior of the EUCLID flash DE as a function of ISS-LIS flash area and maximum group area (MGA) with larger flash DE for those flashes that have a larger optical footprint. Not surprisingly, the flash DE is proportional to the ISS-LIS flash radiance and increases sharply up to an ISS-LIS flash radiance of about 1000 $\mu J/sr/m^2/\mu m$, as demonstrated in Figure 8e. The results

presented above are similar to the ones found by Rudlosky et al. (2017) evaluating the GLD360 DE with respect to TRMM-LIS flash characteristics.

Conversely, the ISS-LIS flash DE can be linked to EUCLID flash characteristics, such as its flash duration, multiplicity and area. To calculate the area of a EUCLID flash the minimum and maximum latitudinal and longitudinal coordinates within the flash are used. Results hereof are presented in Table 4 and distributions drawn in Figure 9. From Fig. 9a it follows that EUCLID flashes with a duration lower than 200 ms have the least chance to match an ISS-LIS flash, resulting in a ISS-LIS flash DE below 60 %. EUCLID flashes lasting longer than 800 ms have an 80 % probability to be matched to an ISS-LIS flash. On average matched EUCLID flashes last twice as long compared to the unmatched flashes. Furthermore, EUCLID flashes have an average multiplicity of 2.4, while this is 2.9 (2.1) for the flashes that match (unmatch) an ISS-LIS flash. For EUCLID flashes with a multiplicity lower than 3, the ISS-LIS flash DE lies between 40-60 %, and increases up to about 70 % for EUCLID flash multiplicities greater than 4, as evidenced in Fig. 9b. Although matched EUCLID flashes have an average area of 25.4 km^2, twice the size of the unmatched EUCLID flashes, the behavior of the ISS-LIS flash DE as a function of EUCLID flash area is not as pronounced, compared to the distributions as a function of EUCLID flash duration and multiplicity.

The diurnal behaviour of the absolute flash detection efficiency for ISS-LIS and EUCLID is plotted in Figure 10. In addition, the ISS-LIS:EUCLID flash ratio is plotted as well. The absolute ISS-LIS flash DE clearly shows an increase at night, compared to daytime, whereas the opposite is noticeable in case of the absolute EUCLID DE. The EUCLID absolute DE drops from about 60 % during [6, 18] UTC to about 50 % within [18, 6] UTC, whereas the ISS-LIS absolute DE increases from about 70 % in between [6, 18] UTC to 75 % within [18, 6] UTC. This behavior is clearly linked to the increased capacity of ISS-LIS to detect more flashes during night time, whilst during the day the flash ratio of ISS-LIS:EUCLID is much closer to one. On the other hand, the performance of EUCLID is expected to be stable throughout the entire day. Hence, the day/night variation depicted in Fig. 10 reflects the limits of the absolute DE calculation, namely it is an upper limit of the true absolute DE.

5 Conclusions

There exists a multitude of different technologies to detect and locate the electrical activity in thunderstorms, whether on a local, continental or global scale. This leads to various sets of observations of the same phenomenon. Hence, depending on the requirements, e.g., spatial accuracy and/or extent, the user can favor one system over the other. Nevertheless, it is important to investigate the similarities and differences among different systems. Incited by the forthcoming launch of the Meteosat Third Generation geostationary satellites, with onboard the Lightning Imager, this study aims at comparing for the first time over a large area in Europe the lightning observations from the ground-based EUCLID network to the optical signals detected by the space-based ISS-LIS. The analysis is based on the lightning activity recorded during March 01, 2017 and March 31, 2019 within the EUCLID network and limited to 54° north. In this study the EUCLID cloud-to-ground

strokes and intracloud pulses are compared to the ISS-LIS groups, in addition to the correlation at the level of the flashes of

320 both systems. Besides measuring the temporal and spatial differences between matched observations a Bayesian approach is adopted to determine the relative and absolute detection efficiencies (DE) of each system where appropriate.

It is found that the matched EUCLID strokes/pulses and ISS-LIS groups are separated by a median distance of 4.8 km, corresponding to approximately two ISS-LIS pixels in the CCD imager. A positive median time difference, $t_{ISS-LIS}$ - t_{EUCLID}, between matched discharges of 0.11 ms is well within the time accuracy of ISS-LIS and indicates that on average the

325 matched ISS-LIS group occurs first. On the other hand, higher peak current signals observed by EUCLID correspond with higher ISS-LIS group radiances. The ISS-LIS group relative DE is 36.5 % overall and 36.6 % in the centre of the EUCLID network. The latter values are in contrast to the much lower EUCLID stroke/pulse relative DE values of 14.7 % and 20.0 % over the full domain and in the centre of the network, respectively. This is related to the higher amount of ISS-LIS groups detected compared to total amount of EUCLID strokes and pulses.

330 On the level of the flashes, the relative ISS-LIS DE is rather homogeneous over the entire EUCLID network with a value of 48.4 %, with the highest values observed at the edge of the EUCLID network, whereas the EUCLID relative DE increases from 45.5 % overall to 56.3 % in the center of the network; related to the increased EUCLID IC:CG flash ratio towards the center of the network. The upper bound of the absolute DE for ISS-LIS drops from 71.3 % overall to 66.1 % in the center of the EUCLID network, whereas in case for EUCLID this value increases from 59.4 % overall to 69.0 % in the center of the

335 network.

The behavior of the relative DE of one system in terms of the flash characteristics of the other reveals that the greater the value, the more likely the other system detects the flash. For instance, it is found that the duration of ISS-LIS flashes is longer by a factor of 1.5 for those that have a match with a EUCLID flash compared to those not observed by EUCLID, while the other way around matched EUCLID flashes last twice as long compared to the unmatched flashes.

340 Finally, the absolute ISS-LIS group and flash DE clearly shows an increase at night, compared to daytime, whereas the opposite is noticeable in case of the absolute EUCLID DE. This behavior is related to the increased capacity of ISS-LIS to detect more flashes during night time, whilst during the day the flash ratio of ISS-LIS:EUCLID is much closer to one.

The main objective of this study was to investigate how well the observations of a ground-based LLS, in this case EUCLID, are linked to space-based optical lightning signatures of LIS on ISS over a large part in western Europe. Consequently, the

345 method described in this work and results thereof provide a framework to be used in potential future studies involving MTG-LI observations over Europe. Moreover, whereas now the focus was on one particular LLS, it is straightforward to apply it to observations of different ground-based LLS covering the entire MTG-LI domain or parts thereof.

Author contribution

350 DRP processed and analyzed the different datasets used in this paper, whereas WS provided feedback along every step in the process. Writing the manuscript was a joint effort of DRP and WS.

Competing interests

The authors declare that they have no conflict of interest.

Acknowledgement

355 Special thanks go to Zhang D., Erdmann F. and Kohlmann H. for benchmarking the scripts used in this work. The authors thank the two anonymous reviewers for their insightful remarks and suggestions.

References

Azadifar, M., Rachidi, F., Rubinstein, M., Paolone, M., Diendorfer, G., Pichler, H., et al. (2016). Evaluation of the performance characteristics of the European Lightning Detection Network EUCLID in the Alps region for upward
360 negative flashes using direct measurements at the instrumented Säntis Tower. *Journal of Geophysical Research: Atmospheres*, *121*(2), 595–606. https://doi.org/10.1002/2015JD024259

Biagi, C. J., Cummins, K. L., Kehoe, K. E., & Krider, E. P. (2007). National Lightning Detection Network (NLDN) performance in southern Arizona, Texas, and Oklahoma in 2003–2004. *Journal of Geophysical Research: Atmospheres*, *112*(D5), D05208. https://doi.org/10.1029/2006JD007341

365 Bitzer, P. M., Burchfield, J. C., & Christian, H. J. (2016). A Bayesian approach to assess the performance of lightning detection systems. *Journal of Atmospheric and Oceanic Technology*, *33*(3), 563–578. https://doi.org/10.1175/JTECH-D-15-0032.1

Blakeslee, R. J. (2019). Non-Quality Controlled Lightning Imaging Sensor (LIS) on International Space Station (ISS) Science Data. NASA Global Hydrology Resource Center DAAC, Huntsville, Alabama, U.S.A.
370 https://doi.org/http://dx.doi.org/10.5067/LIS/ISSLIS/DATA107

Blakeslee, R. J., & Koshak, W. J. (2016). LIS on ISS: Expanded Global Coverage and Enhanced Applications. *The Earth Observer*, *28*(5).

Blakeslee, R. J., Christian, H. J., Stewart, M. F., Mach, D. M., Bateman, M., Walker, T. D., et al. (2014). Lightning Imaging Sensor (LIS) for the International Space Station (ISS): Mission Description and Science Goals. *International*
375 *Conference on Atmospheric Electricity*, (June), 15–20.

Boccippio, D. J., Koshak, W. J., Blakeslee, R. J., Driscoll, K. T., Mach, D., Buechler, D. E., et al. (2000). The Optical

Transient Detector (OTD): Instrument Characteristics and Cross-Sensor Validation. *Journal of Atmospheric and Oceanic Technology*, 441–458.

Boccippio, D. J., Koshak, W. J., & Blakeslee, R. J. (2002). Performance Assessment of the Optical Transient Detector and Lightning Imaging Sensor, Part I. Predicted Diurnal Variability. *Journal of Atmospheric and Oceanic Technology*.

Cecil, D. J., Buechler, D. E., & Blakeslee, R. J. (2014). Gridded lightning climatology from TRMM-LIS and OTD: Dataset description. *Atmospheric Research*, *135–136*, 404–414. https://doi.org/10.1016/j.atmosres.2012.06.028

Christian, H. J., Blakeslee, R. J., & Goodman, S. J. (1989). The detection of lightning from geostationary orbit. *Journal of Geophysical Research: Atmospheres*, *94*(D11), 13329–13337. https://doi.org/10.1029/JD094iD11p13329

Coquillat, S., Defer, E., de Guibert, P., Lambert, D., Pinty, J.-P., Pont, V., et al. (2019). SAETTA: high resolution 3D mapping of the total lightning activity in the Mediterranean basin over Corsica, with a focus on a MCS event. *Atmospheric Measurement Techniques Discussions*, 1–35. https://doi.org/10.5194/amt-2019-192-RC3

Cummins, K. L., Murphy, M. J., Bardo, E. A., Hiscox, W. L., Pyle, R. B., & Pifer, A. E. (1998). A Combined TOA/MDF Technology Upgrade of the U.S. National Lightning Detection Network. *Journal of Geophysical Research*, *103*(D8), 9035. https://doi.org/10.1029/98JD00153

Defer, E., Pinty, J.-P., Coquillat, S., Martin, J. M., Prieur, S., Soula, S., et al. (2015). An overview of the lightning and atmospheric electricity observations collected in southern France during the HYdrological cycle in Mediterranean EXperiment (HyMeX), Special Observation Period 1. *European Geosciences Union (EGU)*, *8(2):649–6*, 649–669. https://doi.org/10.5194/amt-8-649-2015

Diendorfer, G., Pichler, H., & Mair, M. (2009). Some Parameters of Negative Upward-Initiated Lightning to the Gaisberg Tower (2000 - 2007). *Electromagnetic Compatibility, IEEE Transactions On*, *51*(3), 443–452. https://doi.org/10.1109/TEMC.2009.2021616

Ducrocy, V., Braud, I., Davolio, S., Ferretti, R., Flamant, C., Jansa, A., et al. (2013). HyMeX-SOP1, the field campaign dedicated ot heavy precipitation and flash flooding in the northwestern Mediterranean. *American Meteorological Society*, *95*, 1083–1100. https://doi.org/BAMS, 0.1175/BAMS-D-12-00244.1

Enno, S., Sugier, J., Labrador, L. J., & Rudlosky, S. (2018). Comparison and characterisation of ATDnet versus LIS for the period of 2008 to 2014. In *25th International Lightning Detection Conference & 7th International Lightning Meteorology Conference (ILDC/ILMC)* (pp. 1–7). Ft. Lauderdale, Florida, USA.

Erdmann, F., Defer, E., Caumont, O., Blakeslee, R. J., Pédeboy, S., & Coquillat, S. (2019). Concurrent Satellite and ground-based Lightning Observations from the Optical Lightning Imaging Sensor (ISS-LIS), the LF network Meteorage and the SAETTA LMA in the northwestern Mediterranean region. *Atmospheric Measurement Techniques*, (July), 1–32. https://doi.org/10.5194/amt-2019-149

Franklin, V. (2013). *An evaluation of the Lightning Imaging Sensor with new insights on the discrimination of lightning flash and stroke detectability*. University of Alabama in Huntsville.

Goodman, S. J., Buechler, D. E., Wright, P. D., & Rust, W. D. (1988). Lightning and precipitation history of a microburst-

producing storm. *Geophysical Research Letters*, *15*(11), 1185–1188. https://doi.org/10.1029/GL015i011p01185

Heidler, F., & Schulz, W. (2016). Lightning current measurements compared to data from the lightning location system BLIDS. In *International Colloquium on Lightning and Power Systems (CIGRE)*. Bologna, italy.

Jerauld, J. E., Rakov, V. A., Uman, M. A., Rambo, K. J., Jordan, D. M., Cummins, K. L., & Cramer, J. A. (2005). An evaluation of the performance characteristics of the U.S. National Lightning Detection Network in Florida using rocket-triggered lightning. *Journal of Geophysical Research: Atmospheres*, *110*(D19), D19106. https://doi.org/10.1029/2005JD005924

Koshak, W. J. (2010). Optical characteristics of OTD flashes and the implications for flash-type discrimination. *Journal of Atmospheric and Oceanic Technology*, *27*(11), 1822–1838. https://doi.org/10.1175/2010JTECHA1405.1

Mach, D. M., Christian, H. J., Blakeslee, R. J., Boccippio, D. J., Goodman, S. J., & Boeck, W. L. (2007). Performance assessment of the Optical Transient Detector and Lightning Imaging Sensor. *Journal of Geophysical Research: Atmospheres*, *112*(D9), D09210. https://doi.org/10.1029/2006JD007787

Medici, G., Cummins, K. L., Cecil, D. J., Koshak, W. J., & Rudlosky, S. (2017). The Intracloud Lightning Fraction in the Contiguous United States. *Monthly Weather Review*, *145*(11), 4481–4499. https://doi.org/10.1175/MWR-D-16-0426.1

Nag, A., Murphy, M. J., Schulz, W., & Cummins, K. L. (2015). Lightning Locating Systems: Insights on Characteristics and Validation Techniques. *Earth and Space Science*, (2), 65–93. https://doi.org/10.1002/2014EA000051

Orville, R. E., Huffines, G. R., Burrows, W. R., Holle, R. L., & Cummins, K. L. (2002). The North American Lightning Detection Network (NALDN) - First Results : 1998 – 2000. *Monthly Weather Review*, *130*.

Pédeboy, S., Defer, E., & Schulz, W. (2014). Performance of the EUCLID network in cloud lightning detection in the South-East France. In *8th HyMeX Workshop*. Valletta, Malta.

Poelman, D. R., Schulz, W., & Vergeiner, C. (2013). Performance Characteristics of Distinct Lightning Detection Networks Covering Belgium. *Journal of Atmospheric and Oceanic Technology*, *30*(5), 942–951. https://doi.org/10.1175/JTECH-D-12-00162.1

Poelman, D. R., Schulz, W., Diendorfer, G., & Bernardi, M. (2016). The European lightning location system EUCLID – Part 2: Observations. *Natural Hazards and Earth System Sciences*, *16*(2), 607–616. https://doi.org/10.5194/nhess-16-607-2016

Poelman, D. R., Schulz, W., Kaltenböck, R., & Delobbe, L. (2017). Analysis of lightning outliers in the EUCLID network. *Atmospheric Measurement Techniques*, *10*, 4561–4572. Retrieved from https://www.atmos-meas-tech.net/10/4561/2017/

Romero, C., Paolone, M., Rachidi, F., Rubinstein, M., Rubinstein, A., Diendorfer, G., et al. (2011). Preliminary comparison of data from the Säntis Tower and the EUCLID lightning location system. In *2011 International Symposium on Lightning Protection (XI SIPDA)* (pp. 140–145). Fortalzea, Brazil: IEEE. https://doi.org/10.1109/SIPDA.2011.6088468

Rubinstein, M. (1994). On the estimation of the stroke detection efficiency by comparison of adjacent lightning location

445   systems. In *1994 22nd International Conference on Lightning Protection (ICLP)*. Budapest, Hungary.

Rudlosky, S. (2015). Evaluating ENTLN Performance Relative to TRMM / LIS. *Journal of Operational Meteorology*, *3*(2), 11–20. https://doi.org/http://dx.doi.org/10.15191/nwajom.2015.0302.

Rudlosky, S., & Shea, D. T. (2013). Evaluating WWLLN performance relative to TRMM/LIS. *Geophysical Research Letters*, *40*(10), 2344–2348. https://doi.org/10.1002/grl.50428

450   Rudlosky, S., Peterson, M., & Kahn, D. T. (2017). GLD360 performance relative to TRMM LIS. *Journal of Atmospheric and Oceanic Technology*, *34*(6), 1307–1322. https://doi.org/10.1175/JTECH-D-16-0243.1

Schulz, W., Pedeboy, S., Vergeiner, C., Defer, E., & Rison, W. (2014). Validation of the EUCLID LLS during HyMeX SOP1. In *23rd International Lightning Detection Conference & 5th International Lightning Meteorology Conference (ILDC/ILMC)*. Tucson, Arizona, USA.

455   Schulz, W., Diendorfer, G., Pedeboy, S., & Poelman, D. R. (2016). The European lightning location system EUCLID – Part 1: Performance analysis and validation. *Natural Hazards and Earth System Sciences*, *16*(2), 595–605. https://doi.org/10.5194/nhess-16-595-2016

Sparrow, J. G., & Ney, E. P. (1971). Lightning observations by satellite. *Nature*, *232*, 514–540.

Turman, B. N. (1978). Analysis of lightning data from the DMSP satellite. *Journal of Geophysical Research: Oceans*,
460   *83*(C10), 5019–5024. https://doi.org/10.1029/JC083iC10p05019

Vorpahl J A, Sparrow, J. G., & Ney, E. P. (1970). Satellite observations of lightning. *Science*, *169*, 860–862.

Wacker, R. S., & Orville, R. E. (1999). Changes in measured lightning flash count and return stroke peak current after the 1994 U.S. National Lightning Detection Network upgrade: 1. Observations. *Journal of Geophysical Research: Atmospheres*, *104*(D2), 2151–2157. https://doi.org/10.1029/1998JD200060

465   Zhang, D. (2019). Inter-Comparison of Space- and Ground-Based Observations of Lightning. *PhD Thesis*.

Zhang, D., Cummins, K. L., Nag, A., Murphy, M. J., & Bitzer, P. M. (2016). Evaluation of the National Lightning Detection Network Upgrade Using the Lightning Imaging Sensor. In *26th International Lightning Detection Conference & 6th International Lightning Meteorology Conference (ILDC/ILMC)*. San Diego, California, USA.

Zhang, D., Cummins, K. L., Bitzer, P. M., & Koshak, W. J. (2019). Evaluation of the Performance Characteristics of the
470   Lightning Imaging Sensor. *Journal of Atmospheric and Oceanic Technology*. https://doi.org/10.1175/JTECH-D-18-0173.1

475
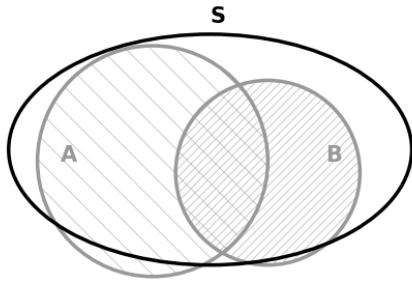
Figure 1. A Venn diagram, illustrating set S as the total amount of occurred lightning discharges, and A and B the set of discharges observed by independent systems. The intersection of A and B is composed of discharges detected by both A and B. Note that there can be a small portion of false alarm discharges detected by either system, that occur outside set S.

480

485
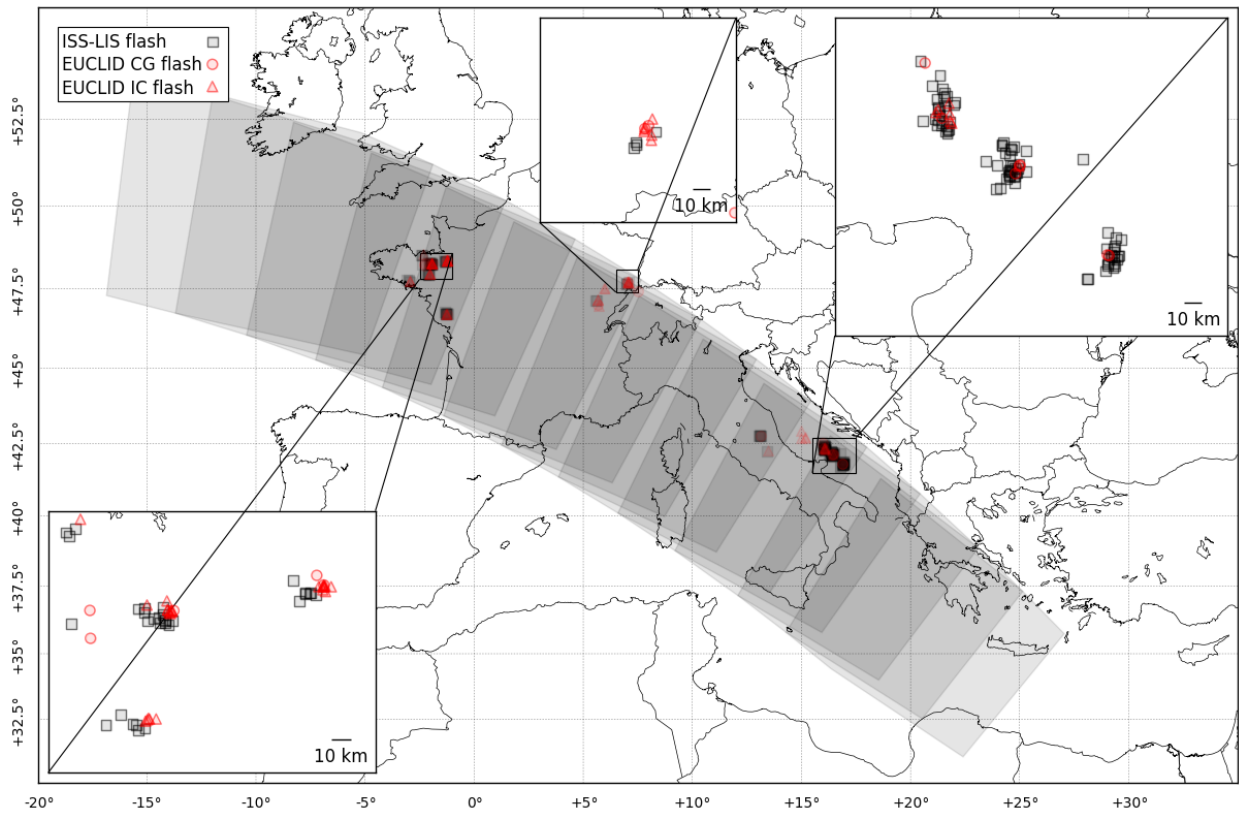
Figure 2. Example of an ISS-LIS track over Europe with the LIS field of view at distinct time steps indicated in gray. Lightning flashes observed by ISS-LIS are displayed, as well as the CG and IC flashes detected by EUCLID.

490

495

500
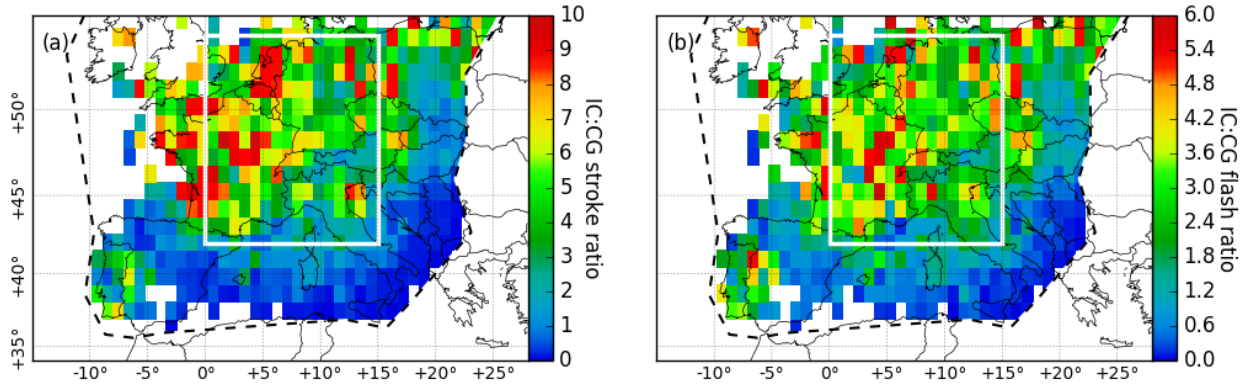
Figure 3. IC:CG (a) stroke and (b) flash ratio within the EUCLID domain (dashed) and cut-off at 54° according to the ISS-LIS maximum latitudonal coverage. The rectangle highlighted in white is the area with the highest IC:CG ratio and is referred to as the centre of the EUCLID network throughout the paper.

505
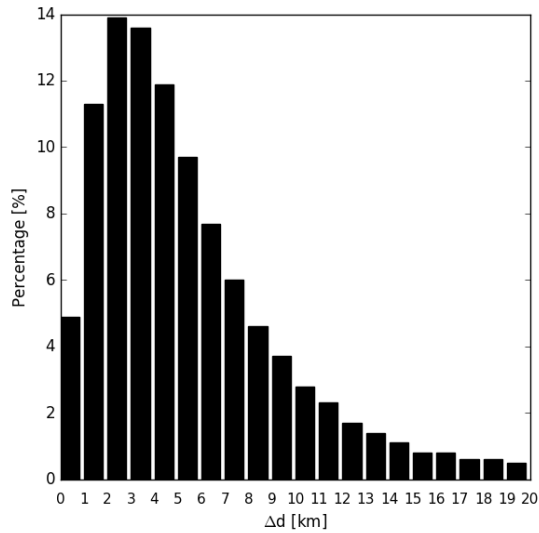
Figure 4. Distance offset between matched ISS-LIS groups and EUCLID strokes/pulses.
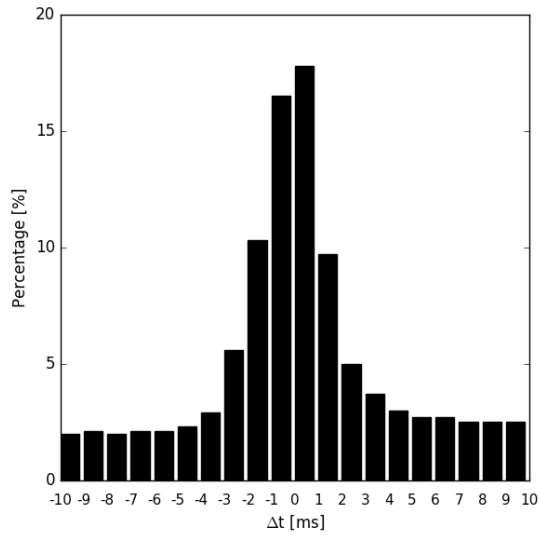
Figure 5. Time offset, $t_{\text{ISS-LIS}} - t_{\text{EUCLID}}$, between matched ISS-LIS groups and EUCLID strokes/pulses. A negative/positive value indicates that the ISS-LIS group occurred earlier/later than the matched EUCLID stroke/pulse.

510
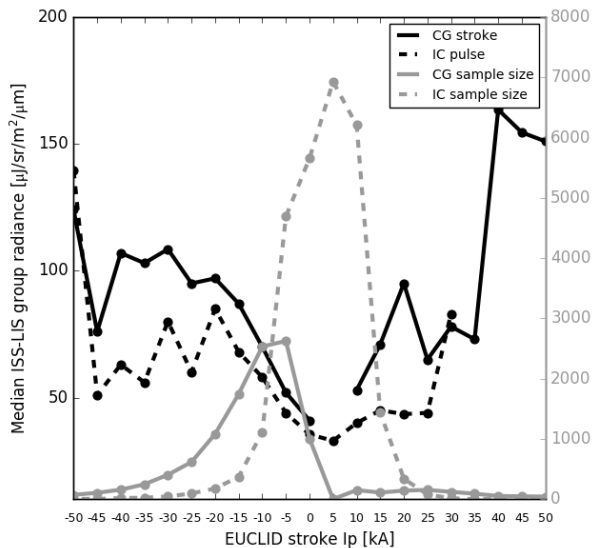
Figure 6. Estimated peak currents of matched EUCLID CG strokes (solid) and IC pulses (dashed) are correlated with the corresponding ISS-LIS group radiance. In general, higher peak current signals are correlated with higher ISS-LIS radiances. In addition, the CG and IC sample size is indicated in grey.
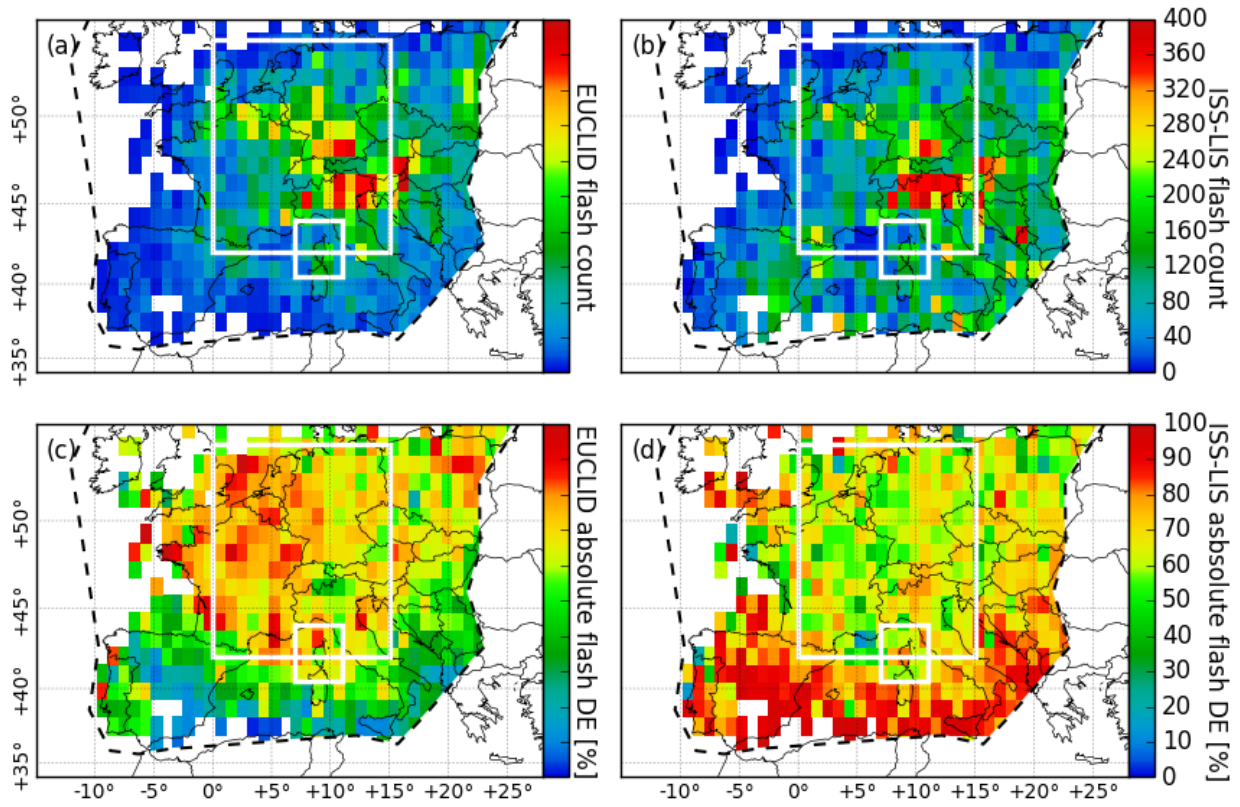
Figure 7. EUCLID and ISS-LIS flash counts are depicted in a) and b), respectively. Plots c) and d) show the spatial distribution of the EUCLID and ISS-LIS absolute detection efficiencies, respectively. The large rectangle highlighted in white is the self-defined centre of the EUCLID network in Figure 3, whereas the smaller white rectangle highlights the area used in Erdmann et al. (2019) against which the results in this paper are compared to.

515

520
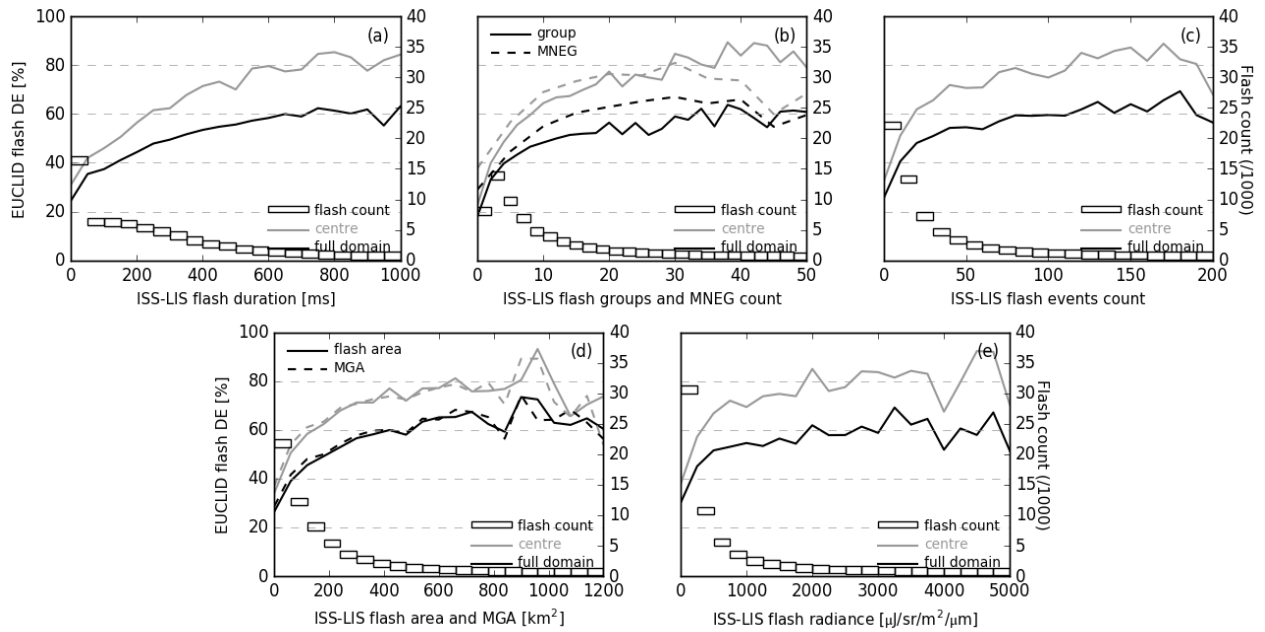
Figure 8. The distribution of EUCLID relative flash DE as a function of ISS-LIS flash characteristics is plotted, such as a) flash duration, b) amount of groups in flash and maximum number of events in a group, c) amount of events, d) flash area and maximum group area and e) flash radiance. Black lines are the results for the full domain, whereas gray lines are related to the centre of EUCLID. Additionally, the ISS-LIS flash counts per interval are plotted as well.
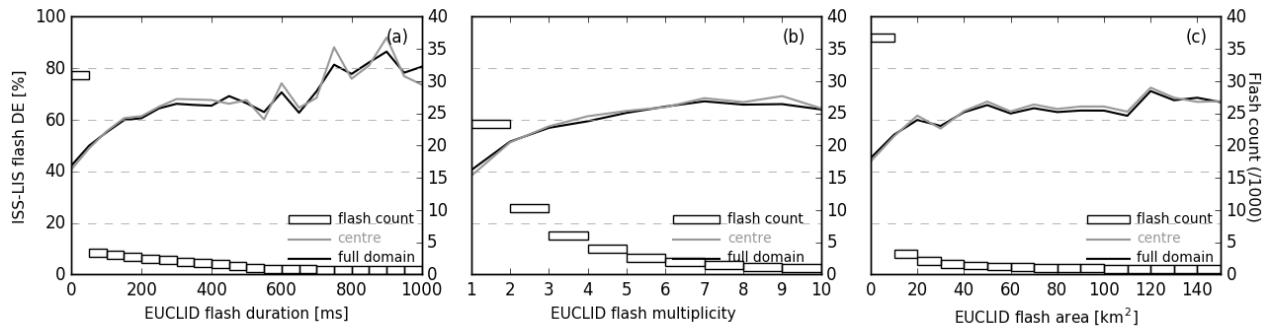
Figure 9. The distribution of ISS-LIS relative flash DE as a function of EUCLID flash characteristics such as flash a) duration, b) multiplicity and c) area. Black lines are the results for the full domain, whereas gray lines are related to the centre of EUCLID. Additionally, the ISS-LIS flash counts per interval are plotted as well.

530
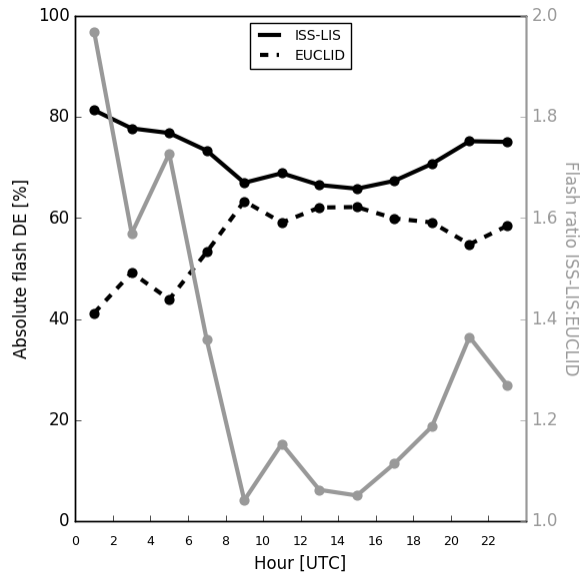
Figure 10. Diurnal distribution of the absolute ISS-LIS (solid) and EUCLID (dashed) flash detection efficiencies. The ISS-LIS:EUCLID flash ratio is indicated in grey.

535

540   TABLE 1: Relative detection efficiencies at the level of EUCLID strokes/pulses and ISS-LIS groups.

	P(EUCLID|ISS-LIS)	P(ISS-LIS|EUCLID)
Full domain	14.7%	36.5%
Centre	20.0%	36.6%

TABLE 2: Relative and absolute flash detection efficiencies for EUCLID and ISS-LIS.

	P(EUCLID|ISS-LIS)	P(ISS-LIS|EUCLID)	P(ISS-LIS)	P(EUCLID)
Full domain	45.5%	48.4%	71.3%	59.4%
Centre	56.3%	48.0%	66.1%	69.0%

545

TABLE 3: Average characteristics of all ISS-LIS flashes, those observed by EUCLID (matched), and those not observed by EUCLID (unmatched).

	ISS-LIS	Matched	Unmatched
Events [count]	28.5	38.2	22.1
Groups [count]	8.6	10.7	7.2
Duration [ms]	210	267.4	172.2
Area [km^2]	172.4	219.8	141.0
MNEG [count]	6.8	8.3	5.8
MGA [km^2]	146.4	186.9	119.6
Radiance [$\mu J/sr/m^2/\mu m$]	579	784	443

MNEG = maximum number of events per group
MGA = maximum group area

550

TABLE 4: Average characteristics of all EUCLID flashes, those observed by ISS-LIS (matched), and those not observed by ISS-LIS (unmatched).

	EUCLID	Matched	Unmatched
Duration [ms]	102.9	136.9	70.5
Multiplicity*	2.4	2.9	2.1
Area [km^2]	18.6	25.4	12.1

*Multiplicity here means the number of strokes, pulses or the sum of both in a pure CG, IC, or hybrid flash, respectively.

555

560

565

570